International Journal of Earth, Energy and Environmental Sciences
ISSN: 2517-942X
Vol:9, No:6, 2015

Production of Composite Materials by Mixing Chromium-Rich Ash and Soda-Lime Glass Powder: Mechanical Properties and Microstructure

Savvas Varitis, Panagiotis Kavouras, George Vourlias, Eleni Pavlidou, Theodoros Karakostas, Philomela Komninou

***Abstract*—**A chromium-loaded ash originating from incineration of tannery sludge under anoxic conditions was mixed with low grade soda-lime glass powder coming from commercial glass bottles. The relative weight proportions of ash over glass powder tested were 30/70, 40/60 and 50/50. The solid mixtures, formed in green state compacts, were sintered at the temperature range of 800°C up to 1200°C. The resulting products were characterized by X-ray diffraction (XRD), scanning electron microscopy (SEM), energy dispersive X-ray spectrometry (EDXS) and micro-indentation. The above methods were employed to characterize the various phases, microstructure and hardness of the produced materials. Thermal treatment at 800°C and 1000°C produced opaque ceramic products composed of a variety of chromium-containing and chromium-free crystalline phases. Thermal treatment at 1200°C gave rise to composite products, where only chromium-containing crystalline phases were detected. Hardness results suggest that specific products are serious candidates for structural applications.

***Keywords*—**Chromium-rich tannery residues, glass-ceramic materials, mechanical properties, microstructure.

I. Introduction

SOLID waste management has been long recognized as one of the most important factors for sustainable development. Despite the fact that research on landfill design and engineering, together with remediation technology, has drawn considerable scientific attention, the main point at issue today is the development and/or improvement of waste management methods for: (a) minimization of disposed residues, (b) minimization of processing costs and (c) production of value added materials. Social pressure, waste legislation, and poor economic context are some of the most important driving forces [1].

One of the most promising methods of waste stabilization/solidification (S/S) is vitrification, i.e. the transformation of solid waste into an inert material, which could be disposed safely or potentially commercialized [2]. The drawback for large scale application of vitrification is its relatively high implementation cost [3].

In this work, we have applied a thermal process where ceramic and composite glass-ceramic end products can be synthesized resembling, in specific cases, those produced by the vitrification method. The process is less energy consuming, since it demands lower thermal treatment temperatures, while the devitrification step, i.e. the secondary thermal treatment step, was avoided. Additionally, cheaper raw materials can be utilized.

Today, almost 90% of global leather production is based on chromium salts for the tanning procedure [4]. During the tanning process 60% of total chromium reacts with raw hides and animal skin, while the remaining 40% is discharged as a liquid by-product. Until recently, 6.5 million tons of wet salted hides were processed [5], producing 300-500 million m^3 of wastewater annually, on global scale [6].

A chromium-loaded ash originating from the incineration of tannery sludge under anoxic conditions was mixed with low grade soda-lime glass powder, in three different proportions, and thermally treated at three different temperatures. In order to evaluate the above process relative to vitrification, the final products were compared to those obtained by the vitrification method applied to the same solid waste [7].

II. Experimental Details

The solid waste was recovered from the industrial zone of Thessaloniki in northern Greece in the form of dried sludge. The sludge was incinerated at anoxic conditions, in order to remove organic carbon, while avoiding oxidation of chromium from the trivalent to the hexavalent form. The by-product of incineration was the chromium-loaded ash (Cr-ash). Details on the pretreatment step and chromium-loaded ash can be found elsewhere [8].

This Cr-ash was mixed with low grade soda-lime glass powder produced from crushed and subsequently pulverized commercial glass bottles. Solid mixtures were pressurized in the form of cylindrical green-state compacts in a uniaxial press. The relative weight proportions of Cr-ash over glass powder tested were 30/70, 40/60 and 50/50. The compacts were thermally treated in an electric furnace (Nabertherm LHT 04/18) with a heat treatment scenario composed of two isothermal steps, each of 30 min duration: the first at 550°C and the second at maximum temperature. Maximum temperatures were 800°C, 1000°C and 1200°C. Each isothermal step was preceded by a temperature increase ramp, of 30 min. As a result, thermal treatment lasted a total of 2 h.. The first isothermal step was imposed in order to remove the remaining organic carbon load [8], and the second for the

S. Varitis, P.Kavouras, G. Vourlias, E. Pavlidou, Th. Karakostas and Ph. Komninou are with the Department of Physics, Aristotle University of Thessaloniki, GR-54124 Thessaloniki, Greece (phone: +30-2310-998195; fax: +30-2310-994314; e-mail: komnhnoy@auth.gr).

occurrence of sintering. Fig. 1 depicts a schematic diagram of the thermal treatment process.

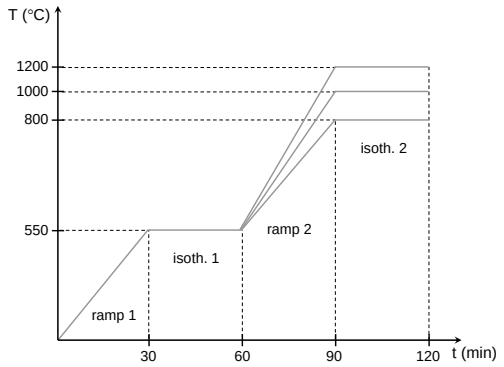

Fig. 1 A Schematic Diagram of Thermal Treatment Steps

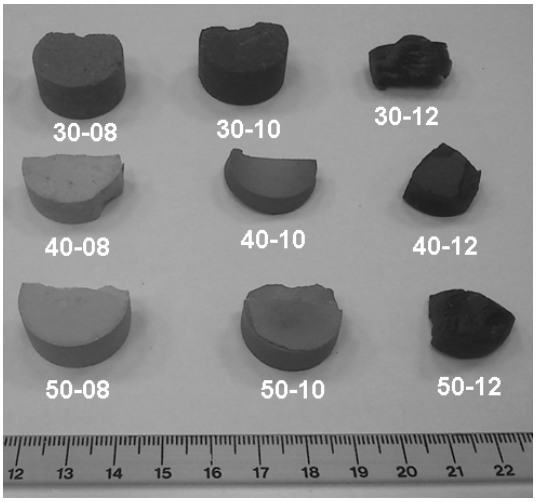

Fig. 2 A General View of All Sintered Products

All sintered products were structurally characterized by X-Ray diffraction (XRD) with a Rigaku powder diffractometer, using CuKa1 radiation. Morphological characterization was made by Scanning Electron Microscopy (SEM) with a JEOL JSM-840A electron microscope. Elemental analysis for all products was made by Energy Dispersive X-ray Spectrometry (EDXS) with an OXFORD ISIS-300 EDS analyzer, attached on the SEM instrument.

Hardness was evaluated by the static micro-indentation technique using a Knoop diamond indenter tip. An Anton Paar MHT-10 indentation tester was used attached on a Zeiss Axiolab-A metallographic microscope. Indentations were performed under 1 N, with 10 s dwell time and 0.2 N/s loading rate. Indentation conditions applied were selected, in order to comply with the following prerequisites: (a) to foster plastic deformation, (b) to create indentation prints with the property of geometric similarity and (c) not produce crack nucleation and propagation. Hardness numbers given in the results part are the mean value of ten indentations.

EDXS analyses and indentation experiments were conducted on mechanically polished surfaces. Polishing was made by wet grinding utilizing SiC papers. The final finishing was achieved with 5.0 μm and 0.3 μm Al_2O_3 pastes. Morphological observations by SEM were conducted on fractured surfaces from the interior of all products.

III. Results

Table I lists composition, thermal treatment conditions and respective code names of the resulting products. Thermal treatment resulted to structurally solid materials, i.e. sintering ensued. The form of all products after sintering is illustrated in Fig. 2.

Structural characterization by XRD showed that sintered products containing 30 wt.% (Fig. 3) and 40 wt.% (Fig. 4) Cr-ash were composed of several different crystalline phases. A common characteristic was the chromium-containing crystalline phases, namely $NaCrSi_2O_6$ (Kosmochlor) and $(Ca_{0.55}Na_{0.45})\cdot(Mg_{0.55}Cr_{0.45})\cdot Si_2O_6$ (Diopsite-Chromian Sodian) for sintering temperatures of 800°C and 1000°C. Table II lists all crystalline phases detected by X-ray diffraction analysis. Chromium-containing phases have been marked with bold letters.

Sintering at 1200°C led to the production of composite products, where only Cr_2O_3 (Eskolaite) crystalline phase was detected. This phase was embedded into an amorphous silicate matrix. This was supported from the fact that at 1200°C, diffraction peaks corresponding to Eskolaite are superimposed onto a characteristic hump, indicative of an X-ray amorphous material (Figs. 3 and 4). Additionally, EDXS elemental analyses showed Si, Ca and Na as the main elements inside the amorphous matrix. Table III lists the complete elemental compositions of the amorphous matrices of 30-12 and 40-12 products. Each number presented there is the mean value of several EDXS point analyses.

The products containing 50 wt.% Cr-ash presented more complicated diffraction patterns, with the following main differences, relative to the other two sets of products described above: (a) additional chromium-containing phases were $Ca_3Cr_2(SiO_4)_3$ (Uvarovite) and $MgCr_2O_4$, (b) sintering at 1200°C did not produce an amorphous matrix. The main similarity with products that contained 30 and 40 wt.% Cr-ash was that Eskolaite was detected after sintering at 1200°C.

SEM observations revealed the morphology of the sintered products, with respect to both Cr-ash content and temperature. Fig. 6 depicts nine SEM micrographs, from all sintered products, where the development of their morphology can be followed. Arrows indicate the increase in sintering temperature for mixtures of the same relative weight ratio of Cr-ash over glass powder.

TABLE I
Code Names of Sintered Products with Respect to Their Composition and Sintering Temperature

Cr-ash/glass powder (mass ratio)	Sintering temperature (°C)		
	800	1000	1200
30/70	30-08	30-10	30-12
40/60	40-08	40-10	40-12
50/50	50-08	50-10	50-12

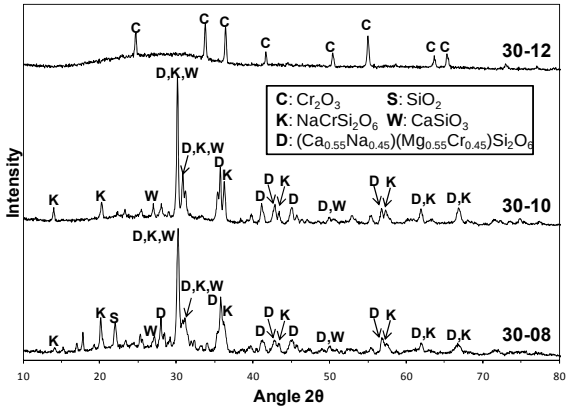

Fig. 3 XRD Diagrams of the Products Containing 30 wt.% Cr-ash

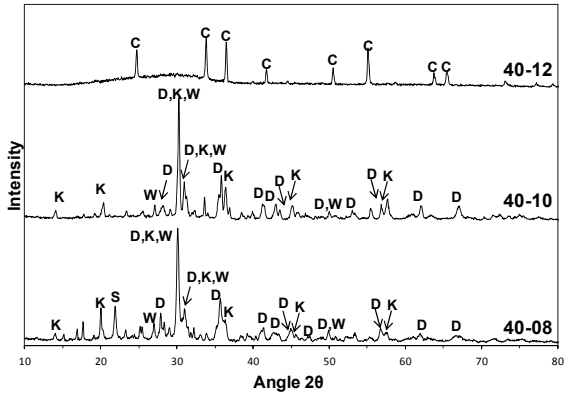

Fig. 4 XRD Diagrams of the Products Containing 40 wt.% Cr-ash. Peak Labels are the same as in Fig. 3

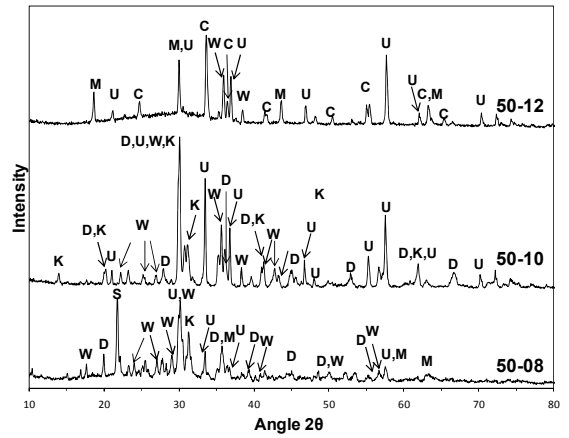

Fig. 5 XRD diagrams of the products containing 50 wt.% Cr-ash. Peak labels are the same as in Fig. 3, with the following additions: U: $Ca_3Cr_2(SiO_4)_6$, M: $MgCr_2O_4$

From Fig. 6 it can be seen that at 800°C fractured surfaces had a granular morphology. Sintering has started homogenizing the solid mixtures, since chromium-loaded ash particles cannot be distinguished from glass powder particles. Increase of Cr-ash weight content from 30% to 50% led to coarsening of the granules. Sintering at 1000°C led to significant alteration of the morphology of 30-10 product; in this case the granules completely disappeared and the product had an appearance more similar of a compact ceramic material. Additionally, pores of irregular shape were developed. Products 40-10 and 50-10 retained the granular morphology of the fractured surfaces, with opposite trends: 40-10 had finer granules, while 50-10 had coarser granules.

At 1200°C products 30-12 and 40-12 had a shiny appearance. As it is shown in Fig. 6 the fractured surfaces were indicative of a glassy material, in agreement to XRD results, where crystalline phases can be distinguished. The pores in these two products had a circular shape, possibly due to inclusion of air. This is an indication that complete melting occurred in these two products at 1200°C.

Product 50-12 had a different morphology; despite the fact that it did not retain the granular morphology, its appearance was less shiny compared to 30-12 and 40-12 products. As it is shown in the respective SEM micrograph, two types of crystallites can be seen: (a) smaller needle -like and (b) larger of circular shape. Since four types of crystallites were detected by XRD (Table II), the background is most possibly composed of crystalline material.

TABLE II
CRYSTALLINE PHASES IN ALL SINTERED PRODUCTS

Ash content (wt.%)	Sintering temperature (°C)		
	800	**1000**	**1200**
30	**$NaCrSi_2O_4$** **Diopsite** SiO_2, $CaSiO_3$	**$NaCrSi_2O_4$** **Diopsite** $CaSiO_3$	**Cr_2O_3**
40	**$NaCrSi_2O_4$** **Diopsite** SiO_2, $CaSiO_3$	**$NaCrSi_2O_4$** **Diopsite** $CaSiO_3$	**Cr_2O_3**
50	**$Ca_3Cr_2(SiO_4)_3$** **$NaCrSi_2O_6$** **Diopsite** SiO_2, $CaSiO_3$	**$Ca_3Cr_2(SiO_4)_3$** **$NaCrSi_2O_6$** **Diopsite** **$MgCr_2O_4$** $CaSiO_3$	**Cr_2O_3** **$Ca_3Cr_2(SiO_4)_3$** **$MgCr_2O_4$** $CaSiO_3$

The chemical formula of Diopsite is $(Ca_{0.55}Na_{0.45})\cdot(Mg_{0.55}Cr_{0.45})\cdot Si_2O_6$.

TABLE III
EDXS ANALYSES FROM THE AMORPHOUS MATRICES OF 30-12 AND 40-12 PRODUCTS IN AT.%

Product	Elements					
	Si	**Ca**	**Na**	**Mg**	**Al**	**Cr**
30-12	61.2	14.4	14.9	6.0	2.2	1.1
40-12	56.3	17.3	16.0	6.6	2.3	1.2

Micro-indentation results are presented in Fig. 7. For sintering at 800°C and 1000°C, only the product with the lowest Cr-ash content could be indented. Measurable indentation marks could not be created in the 40-08, 40-10, 50-08 and 50-10 products. More specifically, indentations removed material, producing a shallow hole of irregular shape with debris around it. The reason was that these products did not acquire the necessary structural integrity, i.e. the ash and glass particles did not have strong physical cohesion.

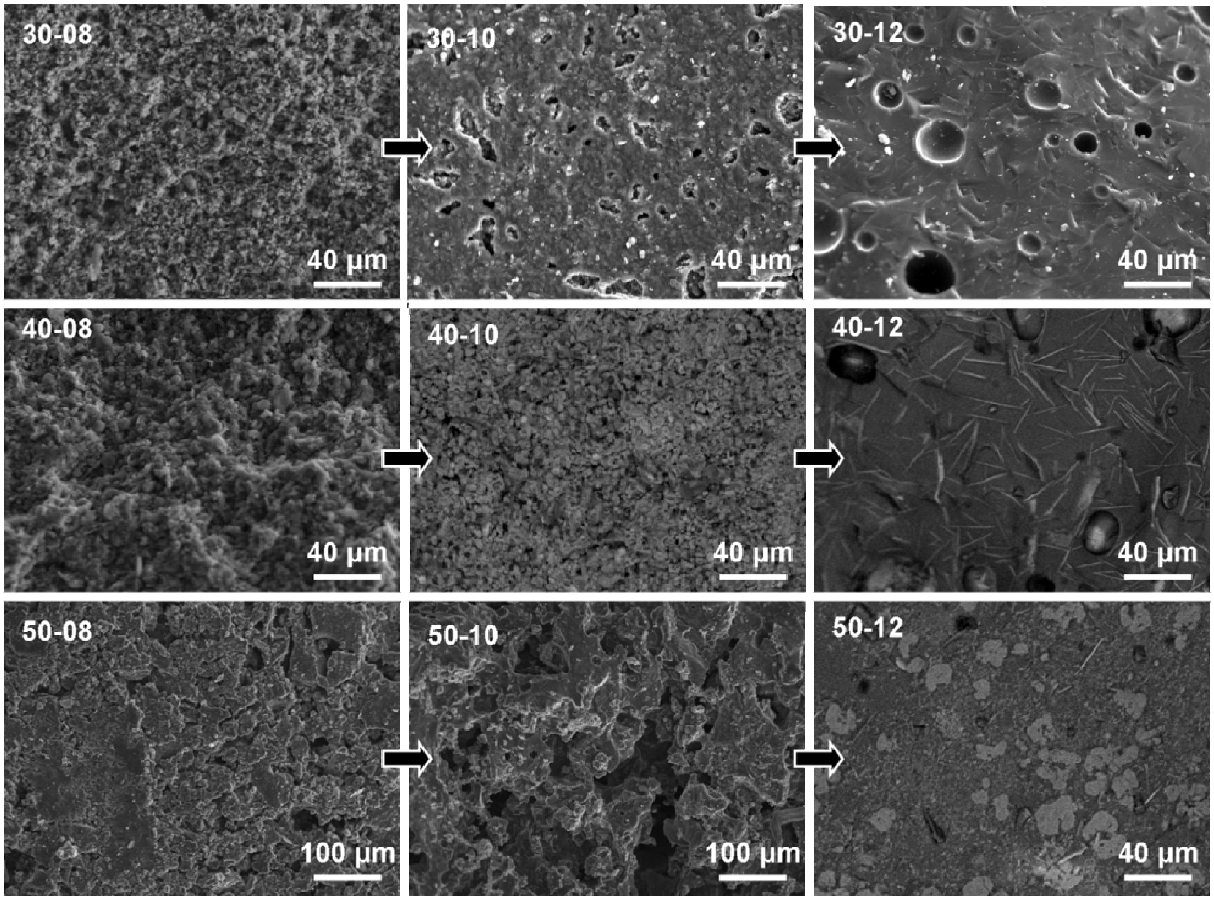

Fig. 6 SEM micrographs obtained from fractured surfaces of all sintered products. The arrows mark sintering temperature increase

The products with the lowest Cr-ash content did have enough structural integrity and as a result measurable indentation prints could give specific results. Product 30-08 gave a hardness number of approximately 1 GPa, while product 30-10 was significantly harder with a hardness number of approximately 5 GPa.

Sintering at 1200°C resulted to materials of comparable hardness numbers, irrespective of Cr-ash content. At this sintering temperature increase of the glass powder content led to a limited increase of hardness number from 4.8 GPa to 5.6 GPa. Additionally, the increase in hardness number between 30-10 and 30-12 products was significantly lower than the increase between 30-08 and 30-10.

IV. Discussion

A. Sintering Process

The sintering products of this work can be categorized in three groups (A, B, C) based on the morphological characteristics as revealed by SEM. This way of categorization was based on the fact that engineering properties such as structural integrity and hardness number were sensitively dependent on morphology.

Group A is composed of the products that showed granular morphology, group B is composed of the products with a typical morphology of a ceramic material and group C is composed of the products that contained amorphous matrix and can be considered as glass-based materials. Products of group A showed relatively poor cohesion between ash and glass particles and various degrees of porosity. Products of group B had better structural integrity relatively to group A products, but lower hardness numbers compared to products of group C.

Table II gives some insight on the progress of sintering process. From 800°C interdiffusion of species between Cr-ash and glass powder has already took place. This assumption is based on the fact that crystalline phases containing silicon and chromium, i.e. elements found only in the glass powder and Cr-ash respectively, have been grown. For example, Diopsite and Kosmochlor gave strong peaks in the respective XRD diagrams. This is in accordance with the observation by SEM that glass powder and ash particles cannot be distinguished. The progress of sintering is further supported from the fact that sintering temperature of 800°C is significantly higher than soda-lime glass transition temperature, which is 570°C [9].

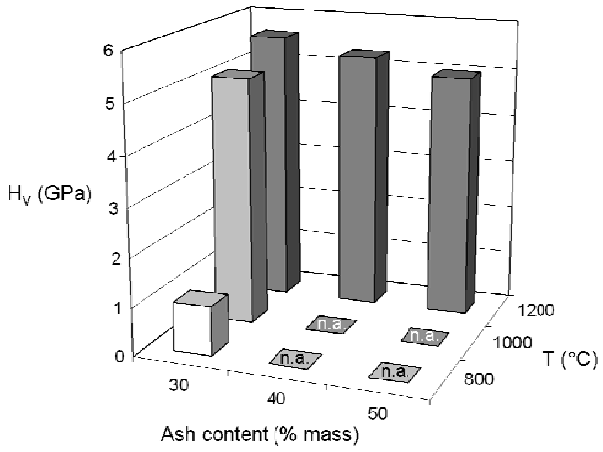

Fig. 7 Hardness number results from all products, obtained with the micro-indentation method (n.a.: not applicable)

Product 30-08 was the only product of group A that indentation experiments could be made. This is obviously due to the higher content in glass powder. Also in product 50-08 a third chromium-containing phase (Uvarovite) has been grown, not detected in 30-08 and 40-08 products. It seems that the relative abundance of chromium, due to the higher content in Cr-ash, led to the formation of this phase. Product 50-10 showed greater degree of porosity than product 50-08. This is possibly a combined effect of: (a) the reduction of glass viscosity and (b) thermal stability of chromium-loaded ash. As a result, glass melt that did not react with the ash has been swollen inside the ash in a mechanical way. The above assumption gives to glass powder the most effective role to solidification at 800°C.

Product 30-10 had a strikingly different morphology, relatively to 40-10 and 50-10. Granular morphology has disappeared, while irregularly shaped pores have been formed. The morphology resembles that of a typical ceramic material obtained from sintering. Relatively high glass powder content has definitely aided at the formation of a compact material, that presented a hardness number close to 5 GPa, i.e. five times harder that 30-08 product. In that case, increase of sintering temperature did not lead to more extensive crystal growth, based on comparison between XRD diagrams of 30-08 and 30-10. Thus, diffusion did not lead to reconstructive transformations in this case, but to further particle coalescence with subsequent porosity coarsening [10].

The above observations do not exclude phase transformations in Cr-ash between 800°C and 1000°C, in products with lower glass powder content. Fig. 5 clearly indicates that crystal growth has taken place in the above temperature interval. More specifically, Uvarovite growth took place since the corresponding peaks increased in intensity, while peaks corresponding to $MgCr_2O_4$ appeared for the first time. These observations underline the relatively less important role of phase transformations in the sintering process (with respect to glass melting), since 50-10 product belongs to group A, i.e. to products with relatively poor structural integrity.

Thermal treatment at 1200°C had a profound influence on the sintering process. Products 30-12 and 40-12 contained only one crystalline phase, Eskolaite, embedded into an amorphous silicate matrix. As a result, at 1200°C sintering process led to glass formation. Eskolaite phase has been observed during vitrification of the same Cr-ash [7], and has been attributed to the relatively limited solubility of chromium in silicate glass matrices [11]. The formation of a silicate glass matrix is responsible for the disappearance of Diopsite-Chromian Sodian, Kosmochlor and Wollastonite crystal phases; the species of those phases were used for the formation of the silicate glass matrix (Table III). The hardness number of these two products was close to that measured by the same method in vitrified lead-containing solid waste products [12].

Finally, product 50-12 did not follow the route of the other two products at 1200°C. Product 50-12 was not a glass-based material, obviously due to the relatively lower content in glass powder. It was a ceramic material, with relatively lower degree of porosity compared to 50-08 and 50-10 due to densification. This is plausibly the reason that the shape of 50-12 product (Fig. 2) was different compared to all other products as it did not retain the cylindrical shape but it significantly deformed due to shrinking.

B. General Remarks

The selection of glass powder as an admixture with the Cr-ash was based on the following arguments: (a) soda-lime glass has a glass transition temperature close to 570°C, and consequently it can act as a binder and/or as a filler in the sintering temperatures applied, aiding solidification, (b) silicate matrices have been proved to stabilize a variety of solid wastes aiding stabilization, (c) the fact that glass already existed in the mixtures could decrease the thermal treatment temperatures, relatively to the standard vitrification method, where glass has to be made from oxide powders of SiO_2, $CaCO_3$ and Na_2CO_3. This process, though, demands melting temperatures of 1400°C or higher [3].

The experimental results presented above show that these arguments have a sound basis. First, glass powder melting seems to have the dominant role in solidifying the Cr-ash, at least at 800°C and 1000°C. Sintered products were ceramics or glass-based products, depending on the sintering conditions and mixture composition. The fact that the increase in glass powder content led to products with better mechanical properties and structural integrity is in favor of its use as a starting material. The morphology and composition of the glass-based products presented above is similar to glass-ceramic products that have been synthesized by the vitrification method for stabilization of the same Cr-ash [7]. This is an indication that chromium in these products has been stabilized, since it participates in the formation of crystalline phases with its trivalent form.

Finally, the sintering process was less energy consuming relative to the vitrification process applied to the same chromium-loaded ash. Temperatures for solidification did not exceed 1200°C, when vitrification temperature was 1400°C

[7]. Sintering temperatures for glass-ceramic production could be potentially further reduced by increasing glass powder content or using glass powder of different composition. Also, no less significant is the fact that the devitrification step demanded for the production of glass-ceramic products was avoided with the sintering process. As a result, processing costs can be further reduced. Fig. 8 depicts a schematic diagram, where a comparison between conventional vitrification of Cr-ash and sintering process applied in this work is made.

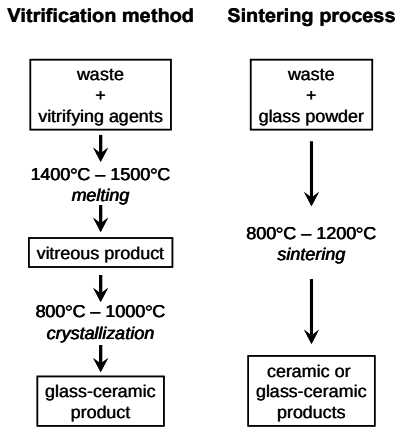

Fig. 8 Comparison of the sintering process applied in this work with the vitrification method process

This work is part of an ongoing research by the authors, in the field of chromium stabilization via the sintering and vitrification methods. Some points of near future research are: (a) further tuning of the sintering conditions and (b) study of the use of other forms of solid wastes for replacement of vitrifying agents (synergistic approach). The stabilization of chromium will be also studied by leaching tests and compared with the performance of the vitrification method.

V. Conclusion

Mixing of Cr-ash with soda-lime glass powder followed by thermal treatment led to the production of: (a) opaque ceramic products composed of chromium-rich and chromium-free crystalline phases at 800°C and 1000°C, and (b) glass-ceramics, i.e. composite products composed of chromium-containing crystalline phases dispersed into a silicate glass matrix at 1200°C. Specific products were found to have hardness numbers between 5.0 GPa to 5.6 GPa and as a result they can be potentially utilized in structural applications. The specific approach, i.e. utilizing glass powder instead of applying the conventional vitrification method poses a number of significant advantages, like lower thermal treatment temperatures, avoidance of the devitrification step and use of lower cost raw materials.

Acknowledgment

This research has been co-financed by the European Union (European Social Fund – ESF) and Greek national funds through the Operational Program "Education and Lifelong Learning" of the National Strategic Reference Framework (NSRF) – Research Funding Program: THALES "WasteVal": Reinforcement of the interdisciplinary and/or inter-institutional research and innovation.

References

[1] M.D. LaGrega, P.L. Buckingham, J.C. Evans, *Hazardous Waste Management*. 2nd ed., New York: McGraw Hill, 2001, ch. 2.
[2] P. Colombo, G. Brusatin, E. Bernardo, G. Scarinci, "Inertization and reuse of waste materials by vitrification and fabrication of glass-based products" *Curr. Opin. Solid State Mater. Sci*., vol. 7, pp. 225-239, Jun. 2003.
[3] J. R. Conner and S. L. Hoeffner, "A critical review of Stabilization/Solidification technology" *Crit. Rev. Environ. Sci. Techol*., vol. 28, pp. 397-462, Sept. 1998.
[4] K. Stein and G. Schwedt, "Chromium speciation in the wastewater from a tannery" *Fresen. J. anal. Chem*., vol. 350, pp. 38–41, Sept. 1994.
[5] J. Kanagaraj, K.C. Velappan, N.K. Chandra Babu, S. Sadulla, "Solid wastes generation in the leather industry and its utilization for cleaner environment - A review" *J. Sci. Indust. Res*., vol. 65, pp. 541–548, Jul. 2006.
[6] J. Jaghava Rao, N.K. Chandrababu, C. Muralidharan, U.N. Balachandran, P.G. Rao, T. Ramasami, "Recouping the wastewater: a way forward for cleaner leather processing" *J. Cleaner Produc*., vol. 11, pp. 591-599, Aug. 2003.
[7] S. Varitis, E. Pavlidou, P. Kavouras, G. Vourlias, K. Chrissafis, A. Xenidis, Th. Karakostas "Devitrification routes of a vitrified chromium-loaded ash" *J. Therm. Anal. Calor*. DOI 10.1007/s10973-015-4539-7 (article in press) 2015.
[8] P. Kavouras, E. Pantazopoulou, S. Varitis, G. Vourlias, K. Chrissafis, G.P. Dimitrakopulos, M. Mitrakas, A.I. Zouboulis, Th. Karakostas, A. Xenidis, "Incineration of tannery sludge under oxic and anoxic conditions: Study of chromium speciation" *J. Hazard. Mater*., vol. 283, pp. 672–679, Febr. 2015.
[9] J. Zarzycki, *Glasses and the vitreous state*. Cambridge: Cambridge University Press, 1991, pp. 12-13.
[10] U. Eisele, "Sintering and hot-pressing" in Materials Science and Technology, vol. 17B, R.J. Brook, Ed. New York: VCH, 1996, pp. 93–96.
[11] H. Khedim, T. Katrina, R. Podor, P.-J. Panteix, C. Rapin, M. Vilasi "Solubility of Cr_2O_3 and speciation of chromium in Soda-Lime-Silicate melts" J. Amer. Ceram. Soc., vol. 93, pp. 1347-1354, Feb. 2010.
[12] P. Kavouras, Ph. Komninou, K. Chrissafis, G. Kaimakamis, S. Kokkou, K. Paraskevopoulos, Th. Karakostas, "Microstructural changes of processed vitrified solid waste products" J. Europ. Ceram. Soc., vol. 23, pp. 1305-1311, Jul. 2003.